1   **Long-term trends and drivers of aerosol pH in eastern China**

2   Min Zhou[1,2], Guangjie Zheng[3], Hongli Wang[1], Liping Qiao[1], Shuhui Zhu[1], Dandan Huang[1], Jingyu An[1],

3   Shengrong Lou[1], Shikang Tao[1], Qian Wang[1], Rusha Yan[1], Yingge Ma[1], Changhong Chen[1], Yafang Cheng[3],

4   Hang Su[*,1,4], Cheng Huang[1]

7   [1]State Environmental Protection Key Laboratory of the Cause and Prevention of Urban Air Pollution

8   Complex, Shanghai Academy of Environmental Sciences, Shanghai200233, China

9   [2]School of Atmospheric Sciences, Nanjing University, Nanjing210023, China

10   [3]Minerva Research Group, Max Planck Institute for Chemistry, Mainz 55128, Germany

11   [4]Multiphase Chemistry Department, Max Planck Institute for Chemistry, Mainz 55128, Germany

13   *Corresponding author: Hang Su (h.su@mpic.de)

20   **Abstract**

21   Aerosol acidity plays a key role in regulating the chemistry and toxicity of atmospheric aerosol particles.

22   The trend of aerosol pH and its drivers are crucial in understanding the multiphase formation pathways

23   of aerosols. Here, we reported the first trend analysis of aerosol pH from 2011 to 2019 in eastern China.

24   The implementation of the Air Pollution Prevention and Control Action Plan leads to -35.8%, -

25   37.6%, -9.6%, -81.0% and 1.2% changes of $PM_{2.5}$, SO_4^{2-}, NH_x, NVCs and NO_3^- in YRD during this

26   period. Different from the fast changes of aerosol compositions due to the implementation of the Air

27   Pollution Prevention and Control Action Plan, aerosol pH shows a moderate change of -0.24 unit over

28   the 9 years. Besides the multiphase buffer effect, the opposite effects of SO_4^{2-} and non-volatile cations

29   changes play key roles in determining the moderate pH trend, contributing to a change of +0.38 and

30   −0.35 unit, respectively. Seasonal variations in aerosol pH were mainly driven by the temperature, while

31   the diurnal variations were driven by both temperature and relative humidity. In the future, SO_2, NO_x

32   and NH_3 emissions are expected to be further reduced by 86.9%, 74.9% and 41.7% in 2050

33   according to the best health effect pollution control scenario (SSP1-26-BHE). The corresponding

34   aerosol pH in eastern China is estimated to increase by ~0.9, resulting in 8% more NO_3^- and 35% less

35   NH_4^+ partitioning/formation in the aerosol phase, which suggests a largely reduced benefit of NH_3 and

36   NO_x emission control in mitigating haze pollution in eastern China.

37

38   **1   Introduction**

39   Aerosol acidity is an important parameter in atmospheric chemistry studies. It affects the particle mass

40   and chemical composition by regulating the reactions of aerosols, and is closely associated with human

41   health, ecosystems and climate(Li et al., 2017; Nenes et al., 2020b; Pye et al., 2020; Su et al., 2020).

42   Aerosol acidity has attracted increasing concern in recent years because of its impacts on the

43   thermodynamics of gas-particle partitioning, pH-dependent condensed-phase reactions and trace metal

44   solubility(Cheng et al., 2016; Fang et al., 2017; Guo et al., 2017b; Guo et al., 2016; He et al., 2018; Song

45   et al., 2018; Weber et al., 2016; Su et al., 2020).

46   Aerosol pH is normally estimated using thermodynamic models, such as E-AIM(Clegg et al., 1998)

47   and ISORROPIA II, due to the limitations of direct aerosol pH measurement techniques(Fountoukis and

48   Nenes, 2007; Hennigan et al., 2015). The global distribution of aerosol pH generally ranges from 1 to

49   6(Pye et al., 2020; Zheng et al., 2020; Su et al., 2020). Aerosols in the United States are highly acidic,

50   with pH values of approximately 1–2(Guo et al., 2015; Nah et al., 2018; Pye et al., 2018; Zheng et al.,

51   2020). Aerosols in mainland China and Europe have similar average aerosol acidity levels (pH = 2.5–

52   6)(Guo et al., 2018; Jia et al., 2018; Masiol et al., 2020; Shi et al., 2019; Tan et al., 2018; Wang et al.,

53   2019; Zheng et al., 2020).

54   Aerosol pH exhibits notable spatial and temporal variability, which is affected by changes in factors

55   such as temperature, relative humidity (RH), and aerosol compositions(Pye et al., 2018; Nenes et al.,

56   2020a; Tao et al., 2020; Zheng et al., 2020). Very few studies have investigated the trend and spatial

57   variability of aerosol pH and its drivers. Weber et al.(Weber et al., 2016) showed that aerosols tend to

58   remain highly acidic upon the reduction of SO_4^{2-} during summertime in the southeastern United States.

59   Based on the 10-year observations in six Canadian sites, Tao and Murphy (Tao and Murphy, 2019)

60   suggested that meteorological parameters are more important than the chemical compositions in

61   controlling aerosol pH variations. Zheng et al.(Zheng et al., 2020) found that aerosol liquid water content

62   (ALWC) and temperature are the main factors that contribute to the pH difference between the wintertime

63   North China Plain and summertime southeastern United States, whereas the change of chemical

64   composition only plays a minor role (15%). In China, the trend of aerosol pH and its drivers remain

65   poorly understood, especially in recent years when the emissions and aerosol compositions undergo

66   substantial changes.

67   To tackle severe particulate matter pollution in China, the Chinese government released the Air

68   Pollution Prevention and Control Action Plan (hereinafter referred to as the Action Plan) in September

69   2013, which is the first plan to specify air quality goals in China(Cai et al., 2017; Liu et al., 2018; Zheng

70   et al., 2018). The implementation of the Action Plan has led to significant changes in the concentrations

71   and chemical characteristics of fine particulate ($PM_{2.5}$). Aerosol pH may change due to the significant

72   changes of the chemical composition in $PM_{2.5}$, which may feedback to the multiphase formation

73   pathways of aerosols such as sulfate, nitrate and ammonium(Cheng et al., 2016).

74   In this study, we performed a comprehensive analysis of the long-term trends of aerosol pH and its

75   drivers in the Yangtze River Delta of eastern China. In this study, a thermodynamic model, ISORROPIA

76   II (version 2.1)(Fountoukis and Nenes, 2007) was applied to estimate the pH based on 9-year continuous

77   online measurements of $PM_{2.5}$ compositions at an urban site in Shanghai. The main purposes of this study

78   were to: (1) characterizing the long-term trend in aerosol pH; (2) investigate the seasonal and diurnal

79   variations of aerosol pH and the main factors that affect these changes and (3) predict further pH under

80   different emission control scenarios and its impact on the formation of ammonium and nitrate. The results

81   presented here may help to advance our understanding of aerosol chemistry in China and support the

82   development of effective pollution control strategy.

83   **2   Material and Methods**

84   **2.1 Ambient measurements**

85   The observational site in this study is located in the Shanghai Academy of Environmental Sciences

86   (SAES, 31°10′N, 121°25′E), a mixed commercial and residential district in the southwest central urban

87   area of Shanghai (Fig. S1). In the absence of a significant nearby industrial source, this sampling site can

88   be regarded as a representative urban area influenced by a wide mixture of emission sources. A detailed

89   description can be found in previous studies(Qiao et al., 2014; Zhou et al., 2016).

90   The sampling was conducted from 2011 to 2019. Hourly mass concentrations of water-soluble gases

91   (HCl, HNO_2, SO_2, HNO_3, NH_3) and major water-soluble inorganic ions in $PM_{2.5}$, including SO_4^{2-}, nitrate

92   (NO_3^-), chloride (Cl^-), ammonium (NH_4^+), sodium (Na^+), potassium (K^+), calcium (Ca^{2+}) and

93   magnesium (Mg^{2+}), were measured using an on-line analyser to monitor aerosols and gases (MARGA

94   ADI 2080, Applikon Analytical B.V). The details of measurements were given in Qiao et al.(Qiao et al.,

95   2014). To better track the retention time changes of different ion species and ensure their concentrations

96   to be measured successfully, an internal calibration was conducted every hour with Lithium Bromide

97   (LiBr) standard solution (Qiao et al., 2014; Zhou et al., 2016). In addition, cleaning the sampling system

98   of MARGA and the multi-points calibrations with the standard solutions were performed every three

99   months to ensure the accuracy of MARGA. Figure S2 compares the sum of SO_4^{2-}, NO_3^- and Cl^- with

100   the sum of NH_4^+, Na^+, K^+, Ca^{2+} and Mg^{2+} in neq/m^3 to check the charge balance. The correlation between

101   cation and anion was strong (R^2=0.94), with a slope of 1.00, indicating that these ion species represented

102   the major ions in $PM_{2.5}$, and the anion and cation were charge balanced. In previous studies,

103   intercomparison experiments between MARGA and filter-based method have been carried out, and the

104   data measured by MARGA show acceptable accuracy and precision(Rumsey et al., 2014; Huang et al.,

105   2014). The mass concentrations of PM$_{2.5}$ were simultaneously measured using an on-line PM monitor

106   (FH 62 C14 series, Thermo Fisher Scientific) using beta attenuation techniques at a time resolution of 5

107   min. The temperature and RH were also measured at a time resolution of 1 min.

2.2 Aerosol pH prediction

109   The aerosol pH was predicted using the ISORROPIA II thermodynamic model(Fountoukis and Nenes,

110   2007). ISORROPIA II can calculate the equilibrium H_{air}^+ and aerosol liquid water content of inorganic

111   material ($ALWC_i$) by inputting the concentrations of the total SO$_4^{2-}$ (TH$_2$SO$_4$, replaced by observed

112   SO$_4^{2-}$), total NO$_3^-$ (TNO$_3$, gas HNO$_3$ plus particle NO$_3^-$), total ammonia (NH$_x$, gas NH$_3$ plus particle

113   NH$_4^+$), total Cl$^-$ (TCl, replaced by observed Cl$^-$ due to the low concentration and measurement

114   uncertainties of HCl)(Rumsey et al., 2014), non-volatile cations (NVCs, observed Na$^+$, K$^+$, Ca^{2+}, Mg^{2+})

115   and meteorological parameters, including temperature and RH(Guo et al., 2016). H_{air}^+ and $ALWC_i$ are

116   then used to obtain the PM$_{2.5}$ pH by Eq. (1).

117    $$pH = -log_{10}H_{aq}^+ \cong -log_{10}\frac{1000H_{air}^+}{ALWC_i+ALWC_o} \cong -log_{10}\frac{1000H_{air}^+}{ALWC_i} \ , \tag{1}$$

118   where H_{aq}^+ is the H$^+$ concentration in solution (mol/L), H_{air}^+ is the H$^+$ loading for an air sample (µg/m^3)

119   and $ALWC_i$ and $ALWC_o$ are the aerosol liquid water contents of inorganic and organic species,

120   respectively (µg/m^3). $ALWC_o$ was calculated by Eq. (2) (Guo et al., 2015).

121    $$ALWC_o = \frac{m_{org}\rho_w}{\rho_{org}}\frac{k_{org}}{(\frac{1}{RH}-1)} \ , \tag{2}$$

122   where m_{org} is the mass concentration of organic aerosol, ρ_w is the density of water (ρ_w=1.0g/cm^3),

123   ρ_{org} is the density of organics (ρ_{org}=1.4g/cm^3)(Guo et al., 2015), and k_{org} is the hygroscopicity

124   parameter of organic aerosol ($k_{org} = 0.087$)(Li et al., 2016). The annual $ALWC_o$ calculated were 1.4–

125   2.5µg/m^3, only accounting for 4.3%–7.5% of the total aerosol liquid water content. The pH predictions

126   in previous studies were insensitive to $ALWC_o$ unless the mass fraction of $ALWC_o$ to the total

127   aerosol liquid water content was close to unity(Guo et al., 2015). The use of $ALWC_i$ to predict pH is

128   therefore fairly accurate and common(Battaglia et al., 2017; Ding et al., 2019). In this study,

129   ISORROPIA II was run in the forward mode and 'metastable' state. Calculations using total (gas and

130   aerosol) measurements in the forward mode are less affected by measurement errors(Hennigan et al.,

131   2015; Song et al., 2018). A detailed description of the pH calculations can be found in previous

132   studies(Guo et al., 2017a; Guo et al., 2015; Song et al., 2018).

133   Figure S3 compares the predicted and measured concentrations of NH_3, NH_4^+, NO_3^- and HNO_3. The

134   results show that the modelled and measured NH_3, NH_4^+ and NO_3^- concentrations are in good agreement,

135   with R^2 values above 0.89 and slopes near 1.00, indicating that the thermodynamic analysis accurately

136   represents the aerosol state and that deviations in the calculated pH values are lower than that in modelled

137   NH_3[Weber et al., 2016]. However, the predicted and measured concentrations of HNO_3 show a poor correlation,

138   as reported in previous studies(Ding et al., 2019; Guo et al., 2015). This may be attributed to lower gas-

139   phase concentrations than particle-phase concentrations and the measurement uncertainties of HNO_3

140   from MARGA(Rumsey et al., 2014). The development of an alternative approach is therefore required

141   to accurately represent HNO_3.

142   **2.3 Sensitivity analysis and drivers of aerosol pH**

143   To investigate the factors that drive changes in aerosol pH, sensitivity tests of pH to different factors,

144   including temperature, RH, SO_4^{2-}, TNO_3, NH_x, Cl^- and NVCs, were performed. Figure S4 shows how

145   these factors affected the aerosol pH. In the sensitivity tests, we found that an elevated temperature and

146   SO_4^{2-} could decrease pH. As shown in Figure S4, particles tend to become more acidic at higher

147   temperatures. The temperature dependence of pH is mainly determined by the phase partitioning of

148   NH_3/NH_4^+ based on the equilibria $NH_3\,(g) \leftrightarrow NH_3\,(aq)$ and $NH_3\,(aq) + H_2O \leftrightarrow NH_4^+ + OH^-$, which are

149   governed by the temperature-dependent constants K_H and K_b, respectively(Hennigan et al., 2015; Zheng

150   et al., 2020). Figures S4 also show that elevations in NH_x, NVCs and RH can increase the aerosol pH

151   and ALWC. For TNO_3 and Cl^-, we find their impacts on the aerosol pH were rather weak through

152   sensitivity test and thus are not discussed in detail here.

153   In this study, we also try to quantify the effects of different factors on the annual, seasonal and

154   diurnal variations of aerosol pH to identify the most important determinants. To quantify the effects of

155   individual factors on the aerosol pH, we first estimated the pH by using the ISORROPIA model with

156   initial values of the different factors, including annual, seasonal and hourly mean value of temperature,

157   RH, SO_4^{2-}, TNO_3, NH_x, Cl^- and NVCs. We then estimated the changed pH (pH_{change}) by varying one

158   factor while holding the other factors fixed. The difference in aerosol pH (ΔpH, $\Delta pH = pH_{change} - pH$)

159   represents the effect of an individual factor change on the aerosol pH.

160   **3   Results and Discussion**

161   **3.1 Long-term trends of aerosol pH**

162   **3.1.1 Trends of aerosol pH.**

163   The 9-year time series of aerosol pH calculated by ISORROPIA II is shown in Figure 1a. A declining

164   trend in $PM_{2.5}$ pH from 3.30 ± 0.58 in 2011 to 3.06 ± 0.55 in 2019 was observed, with the fitted decrease

165   rate of around 0.04 unit pH per year, which may be related to chemical composition changes (Figs. S5-

166   S6) due to the pollution control measures taken in the Yangtze River Delta (YRD) region. The Chinese

167   government started to implement the Action Plan, a series of air pollution control policies, in September

168   2013, which resulted in a clear decline in $PM_{2.5}$ and its chemical components(Cheng et al., 2019; Li et

169   al., 2019). Compared to the concentrations before the implement of the Action Plan (i.e., 2011-2012

170   averages), $PM_{2.5}$, SO_4^{2-}, NH_x and NVCs after the implement of the Action Plan (i.e., 2018-2019 averages)

171   decreased by 35.8%, 37.6%, 9.6% and 81.0%, respectively, while NO_3^- increased by 1.2% (Fig. S5). In

172   terms of the chemical profiles, SO_4^{2-}, NH_4^+ and NO_3^- remain the most abundant inorganic water-soluble

173   ions, accounting for 83.4%–94.1% of the total ions in $PM_{2.5}$. While the proportions of NH_4^+ and NO_3^-

174   increased continuously (increased by 2.2% and 13.1% from 2011 to 2019, respectively), those of NVCs

175   and SO_4^{2-} decreased by 6.0% and 4.6%, respectively. Despite of the substantial change of aerosol

176   abundance and composition, the aerosol pH shows a moderate change. The effects of chemical

177   composition changes in $PM_{2.5}$ on the aerosol pH are further discussed in Section 3.1.2.

178   The $PM_{2.5}$ in Shanghai was moderately acidic with daily pH range from 1.15 to 5.62, similar to

179   those from other cities in China(Shi et al., 2019; Tan et al., 2018). Table S1 shows the pH data from the

180   literature, which were calculated using thermodynamic models of different cities in summer and winter.

181   In general, the $PM_{2.5}$ pH ranges in Chinese cities were higher than those in US cities yet similar to those

182   in European cities.

183   **3.1.2 Driving factors.**

184   Figure 1b shows the contributions of individual factors to the ΔpH from 2011 to 2019. Note that in Fig.

185   1b, the aerosol pH was calculated from the annual averages of input parameters. This is different from

186   Sect 3.1.1, where the annual pH is the average of hourly values based on hourly observation data. The

187   aerosol pH decreased from 3.35 in 2011 to 3.28 in 2013. The main factors that affected the pH in this

188   period (prior to the implementation of the Action Plan) were the temperature and NVCs. Upon

189   implementation of the Action Plan (2013-2019), the concentrations of $PM_{2.5}$ and its chemical components

190   decreased substantially (Fig. S5); hence, the role of the chemical composition in the aerosol pH become

191   more prominent than the period of 2011-2013. The pH value continuously decreased from 3.28 in 2013

192   to 3.19 in 2019. Changes in SO_4^{2-} and NVCs were more important determinants of the change of aerosol

193   pH, resulting in ΔpH of +0.38 units and −0.35 units from 2013 to 2019, respectively. Besides the effect

194   of reduction in SO_4^{2-} (Fu et al., 2015; Xie et al., 2020), our results suggest that the change in NVCs may

195   also play an important role in determining the trend of aerosol pH. The effects of SO_4^{2-} and NVCs on pH

196   were much weaker during 2017–2019 than during 2013–2017, consistent with the fact that the decline in

197   pollutant concentrations has slowed in recent years (Fig. S6). Thus, temperature and NH_x become the

198   main drivers of the ΔpH during 2017–2019.

199   From 2013 to 2019, changes in the NH_x and Cl^- were associated with 0.08 and 0.06 decreases in

200   ΔpH, respectively, whereas TNO_3 had little effect on the ΔpH. Overall, the changes in SO_4^{2-} and NVCs

201   were the main drivers of the ΔpH under the implemented Action Plan, and NH_x appeared to play an

202   increasingly important role in determining the aerosol pH through the years.

203
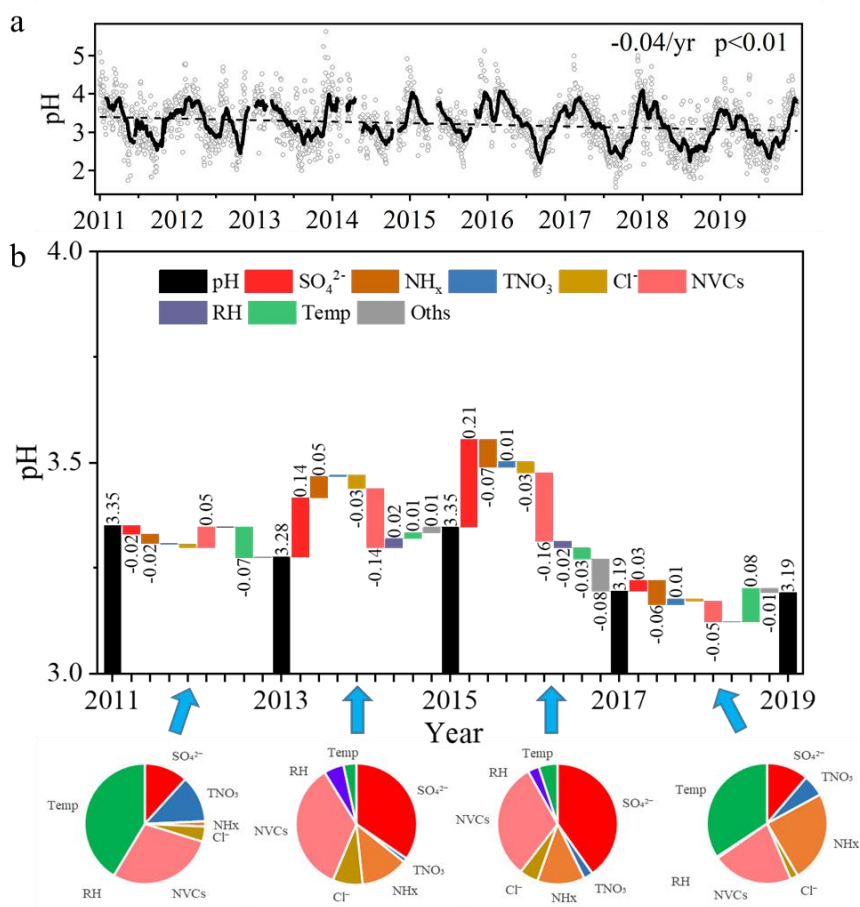
Figure 1. (a) Long-term trends in aerosol pH during 2011–2019 in Shanghai. Gray dots and black lines

represent the daily pH values and 30-day moving average pH values, respectively. (b) Fractional

contribution of individual drivers to the change in aerosol pH during 2011–2019. RH, relative humidity;

Temp, temperature; NVCs, non-volatile cations; NH_x, total ammonia; TNO_3, total nitrate.

3.2 Seasonal variation

Figure 2 shows the seasonal variations of aerosol pH in Shanghai. The average pH values were 3.33±

0.49, 2.89 ± 0.49, 2.99 ± 0.52 and 3.59 ± 0.57 in spring (March–May, MAM), summer (June–August,

JJA), fall (September–November, SON) and winter (December–February, DJF), respectively. The

highest aerosol pH was found in winter while the lowest pH was found in summer. This is with similar

seasonal trend but generally lower levels than that observed in Beijing and other NCP cities (Tan et al.,

214   2018; Ding et al., 2019; Shi et al., 2019; Wang et al., 2020), due to the generally lower aerosol

215   concentrations in YRD.

216   According to the multiphase buffer theory, the peak buffer pH, pK_a^* regulates the aerosol pH in a

217   multiphase-buffered system, and temperature can largely drive the seasonal variation of aerosol pH

218   through its impact on pK_a^*(Zheng et al., 2020). Figure 3 confirms this conclusion, and shows a dominant

219   role of temperature in driving the seasonal variation of aerosol pH. The temperature was associated with

220   a max ΔpH of 0.63 from fall to winter. Besides temperature, the main factors affecting aerosol pH are

221   NH_x and SO_4^{2-} (Fig. 3), contributing 16% and 12% of the changes, respectively. Our results suggest a

222   central role of temperature in the determination of seasonal variations in aerosol pH, consistent with the

223   results of Tao and Murphy (Tao and Murphy, 2019) at six Canadian sites and the prediction by the

224   multiphase buffer theory(Zheng et al., 2020). In comparison, some previous studies emphasized the

225   importance of chemical compositions in seasonal variations (Tan et al., 2018; Ding et al., 2019), which

226   is mainly due to the different sensitivity analysis methods applied.

227

228
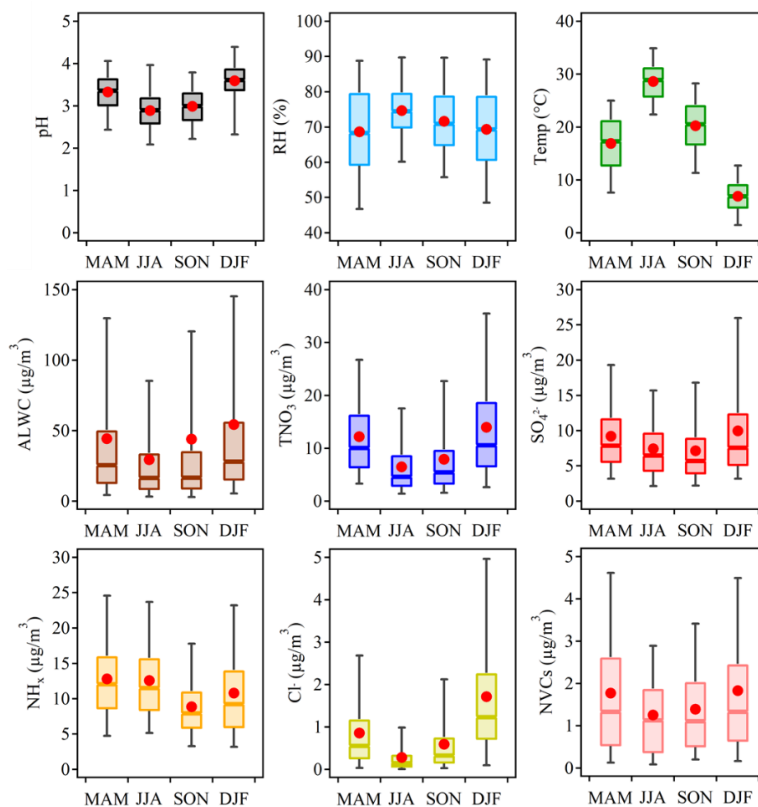
Figure 2. Seasonal patterns of the mass concentrations of major components in PM2.5, relative humidity (RH),

230

temperature (Temp), predicted aerosol liquid water content (ALWC) and aerosol pH during 2011–2019 in

231

Shanghai.
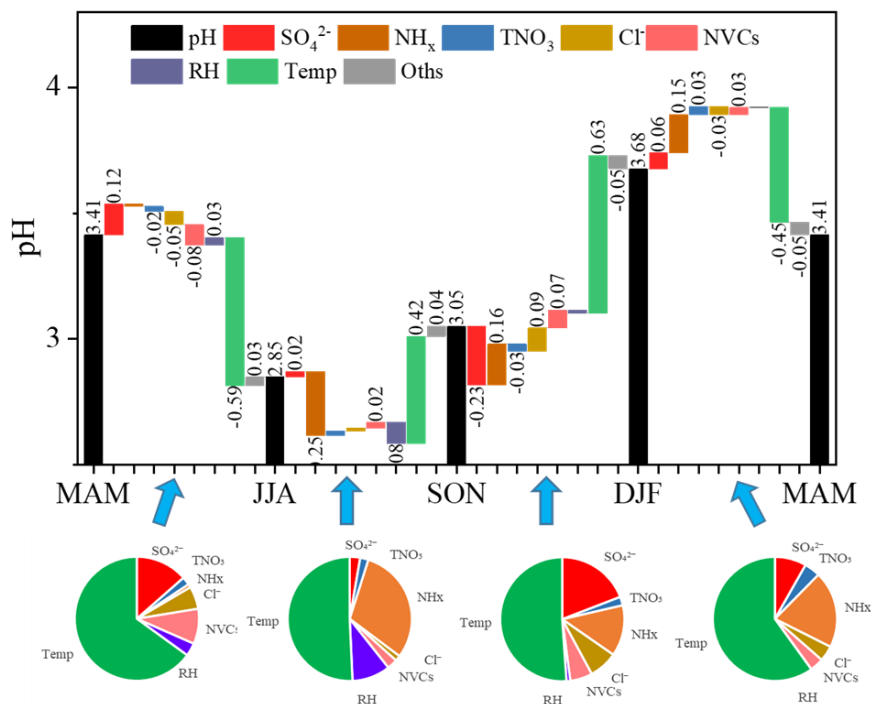
Figure 3. Fractional contributions of individual drivers to the changes in aerosol pH across the four seasons.

RH, relative humidity; Temp, temperature; NVCs, non-volatile cations; NH$_x$, total ammonia; TNO$_3$, total

nitrate.

3.3 Diurnal variation

Figure 4 shows the diurnal variations in the aerosol pH and its potential drivers. Similar to the results in Beijing(Tao et al., 2020), aerosol pH in Shanghai exhibits notable diurnal variations, being higher during nighttime.

Figure 5 shows the effects of individual factors on the diurnal variations in aerosol pH. Temperature and RH are among the main drivers of this diurnal variation of aerosol pH, with a max ΔpH of -0.22 and +0.10 units. As shown in Fig. 4, the maximum RH and ALWC occurred at approximately 5:00. After sunrise, increase of temperature resulted in an immediate drop of RH and ALWC with ALWC reached its lowest level in the afternoon. Accordingly, the minimum aerosol pH (~2.8) was also found in the afternoon with high temperature and low RH. After sunset, the decreasing temperature and increasing

246   RH led to a highest aerosol pH overnight. Minor pH changes were found between 0:00 and 6:00, when

247   temperature and RH also show minor changes. The effects of other factors on the diurnal variations in

248   pH were notably smaller than their effects on seasonal variations, which may be attributed to the

249   relatively small variations of chemical profiles in the course of a day. Among these chemical factors,

250   NH_x plays the most important roles, followed by SO_4^{2-}. Overall, temperature and RH are more important

251   than the chemical compositions in controlling the diurnal variations in aerosol pH.
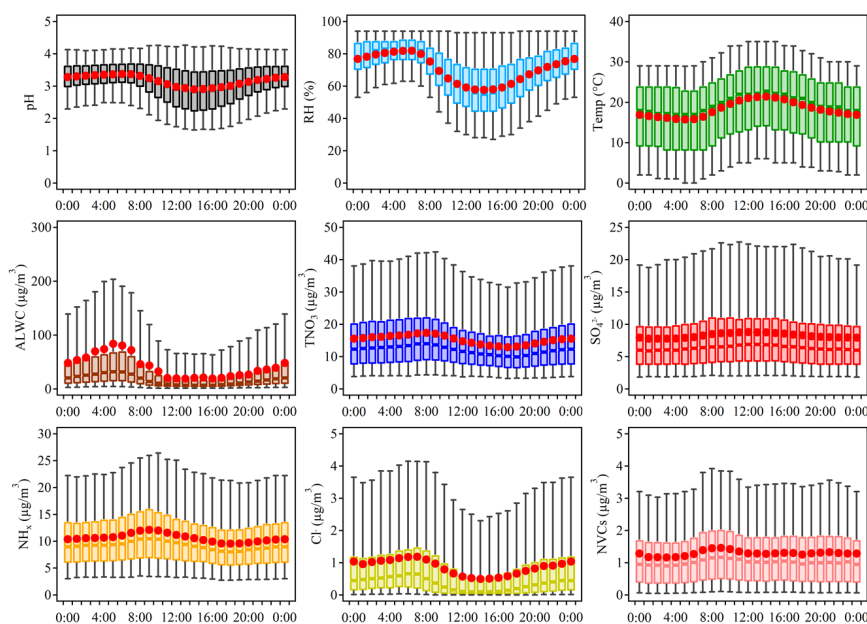
252

253   **Figure 4. Diurnal patterns of the mass concentrations of major ions in PM$_{2.5}$, relative humidity (RH),**

254   **temperature (Temp), predicted aerosol liquid water content (ALWC) and aerosol pH during 2011–2019 in**

255   **Shanghai.**

256
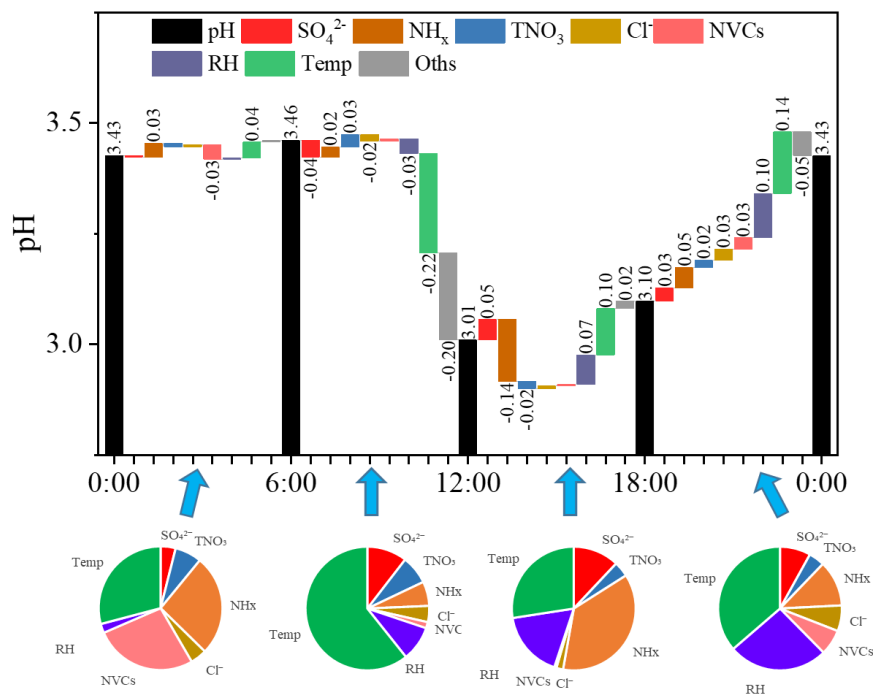
Figure 5. Fractional contributions of individual drivers to the aerosol pH difference between day and night. RH, relative humidity; Temp, temperature; NVCs, non-volatile cations; NH$_x$, total ammonia; TNO$_3$, total nitrate.

3.4 Future projections

A series of prevention and control measures are suggested for continuous improvement of air quality, which will affect the atmospheric compositions and may subsequently affect the aerosol pH in China. To explore China's future anthropogenic emission pathways in 2015–2050, Tong et al.(Tong et al., 2020) developed a dynamic projection model, based on which different emission scenarios were created by connecting five socio-economic pathway (SSP) scenarios, five representative concentration pathways (RCP) scenarios (RCP8.5, 7.0, 6.0, 4.5 and 2.6) and three pollution control scenarios (business as usual, BAU; enhanced control policy, ECP; and best health effect, BHE). These scenarios provide a better understanding of the future trends in pollutant emissions(Tong et al., 2020).

In this study, we chose three different emission reduction scenarios as the future anthropogenic

271 emission pathways, including SSP3-70-BAU, SSP2-45-ECP and SSP1-26-BHE, and tried to project the

272 future aerosol pH levels in Shanghai. SSP1-26-BHE, which involves a combination of strong low-carbon

273 and air pollution control policy, has the greatest emission reduction, followed by SSP2-45-ECP. SSP3-

274 70-BAU is a reference scenario without any active actions. Figure 6 shows the emissions of SO_2, NO_x

275 and NH_3 and predicted pH levels in China from 2015 to 2050 under the three scenarios. We also predicted

276 the aerosol pH based on the assumption that reductions in SO_4^{2-}, TNO_3 and NH_x are equivalent to

277 reductions in their respective precursors (i.e., SO_2, NO_x and NH_3).

278   As shown in Fig. 6, the future trend of aerosol pH changes little under the weak control policy

279 (SSP3-70-BAU). Correspondingly, there is also little change in the predicted NO_3^- partition ratio (NO_3^-/

280 (NO_3^- + HNO_3)). However, NH_4^+ partition ratio (NH_4^+/(NH_4^+ + NH_3)) increases substantially, suggesting

281 an enhanced formation of ammonium aerosols. Under the moderate control policy (SSP2-45-ECP), the

282 emissions of SO_2, NO_x, and NH_3 in 2050 will be reduced by 62.7%, 49.0% and 25.0%, respectively. This

283 would result in an increase in pH of ~0.5, while the decreases in NO_3^- and NH_4^+ partition ratios of 0.14

284 and 0.23 respectively. That is, more nitrate and ammonium will exist in the gas phase as HNO_3 and NH_3.

285 With the strict control policy (SSP1-26-BHE), the emissions of SO_2, NO_x and NH_3 in 2050 will be

286 reduced by 86.9%, 74.9% and 41.7%, respectively, and the pH will further increase to 4.30 in 2050. It is

287 noted that the predicted pH values in the SSP1-26-BHE model decrease suddenly during 2030–2040 and

288 then continue to rise, which is due to the decrease in ALWC and increase in pH brought by the decrease

289 of SO_4^{2-}, TNO_3 and NH_x during 2015-2030. These variations result in a transition to the HNO_3-sensitive

290 regime during 2030-2040, where partitioning gradually shifts from aerosol-phase nitrate to the gaseous

291 phase(Nenes et al., 2020a). Therefore, the decrease in TNO_3 during 2030–2040 lead to a notable decrease

292 of pH. This can also be seen from Fig. 6e, where NO_3^- partition ratio begins to decrease gradually and

293 reaches the HNO_3-sensitive regime and then rises again under the strict control policy, resulting in NO_3^-

294 partition ratio increased from 0.92 in 2015 to 1.00 in 2050. According to the strict control policy, we also

295 found that NH_4^+ partition ratio has dropped significantly from 0.37 in 2015 to 0.02 in 2050. Because of

296 China's commitment in reducing CO_2, we expect a further roadmap of emission control similar to the

297 SSP1-26-BHE scenario. In this case, the corresponding aerosol pH in eastern China will increase by ~0.9,

298 resulting in 8% more NO_3^- and 35% less NH_4^+ partitioning/formation in the aerosol phase. This would

299 suggest a largely reduced benefit of NH_3 and NO_x emission control in mitigating haze pollution in eastern

300   China.

301
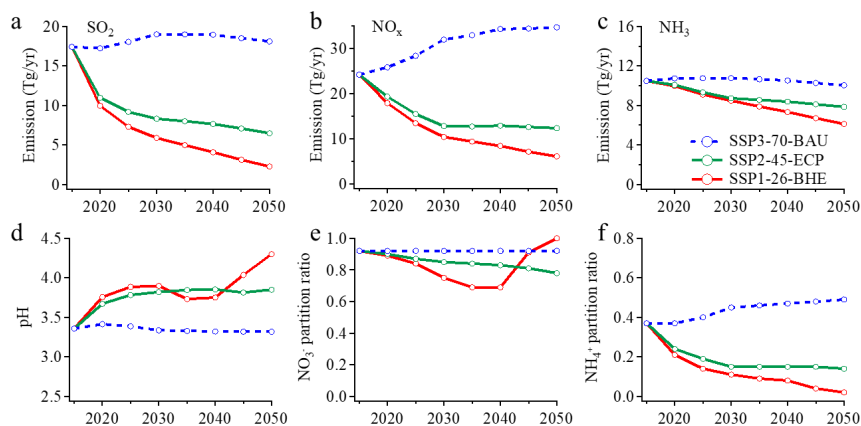
Figure 6. Emissions of SO$_2$ (a), NO$_x$ (b), NH$_3$ (c), predicted pH (d), NO$_3^-$ partition (NO$_3^-$ / (NO$_3^-$ + HNO$_3$)) (e)

and NH$_4^+$ partition (NH$_4^+$ / (NH$_4^+$ + NH$_3$)) (f) in China from 2015 to 2050 under the three scenarios published

in Tong et al.(Tong et al., 2020)

305

4   Conclusion

The aerosol pH values at an urban site in Shanghai during 2011–2019 were calculated using ISORROPIA

II. The aerosol pH decreased from 3.30 ± 0.58 in 2011 to 3.06 ± 0.58 in 2019, which is related to changes

in the chemical composition under the implementation of Action Plan in the YRD region. The

implementation of the Action Plan leads to -35.8%, -37.6%, -9.6%, -81.0% and +1.2% changes in

concentrations of PM$_{2.5}$, SO$_4^{2-}$, NH$_x$, NVCs and NO$_3^-$ in YRD during this period. Then we quantified the

contributions of individual factors to the difference in aerosol pH from 2011 to 2019. Before the

implementation of the Action Plan (2011-2013), the main factors that affected the pH were the

temperature and NVCs. During the implementation of the Action Plan (2013-2019), SO$_4^{2-}$ and NVCs

were the most important determinants of the aerosol pH and were attributed to ΔpH of +0.38 and −0.35

units, respectively. Meanwhile, changes in NH$_x$ and Cl$^-$ were responsible for decreases in aerosol pH of

0.08 and 0.06 pH units, respectively, whereas the effect of TNO$_3$ was negligible. NH$_x$ appeared to play

an increasingly important role in determining aerosol pH through the years.

319   Distinct seasonal variations in the aerosol pH were observed, with maximum and minimum aerosol

320   pH of 3.59 ± 0.57 in winter (DJF) and 2.89 ± 0.49 in summer (JJA), respectively. Temperature through

321   its impact on pKa* can largely drive the seasonal variation of aerosol pH in a multiphase-buffered system.

322   Besides temperature, the main factors affecting the seasonal variation of aerosol pH are NH_x and SO_4^{2-},

323   which contributed to +16% and +12% pH change, respectively. The diurnal cycle of particle pH is driven

324   by the combined effects of temperature and relative humidity with a maximum ΔpH of -0.22 and +0.10

325   units, respectively. The effects of chemical factors on the diurnal variations in pH were notably smaller

326   than the effects on seasonal variations, which may be attributed to the limited variations of chemical

327   profiles in the course of a day.

328   Finally, to explore the effects of China's future anthropogenic emission control pathways on aerosol

329   pH and compositions, we chose three different emission reduction scenarios proposed by Tong et

330   al.(Tong et al., 2020) for future haze mitigation, naming SSP3-70-BAU, SSP2-45-ECP and SSP1-26-

331   BHE as case studies. We estimated that the future trend of aerosol pH and NO_3^- partition ratio change

332   little under the weak control policy (SSP3-70-BAU). However, NH_4^+ partition ratio increases

333   substantially, suggesting an enhanced formation of ammonium aerosols. The results also demonstrate

334   that future aerosol pH will increase under both strict control policy (SSP1-26-BHE) and moderate control

335   policy (SSP2-45-ECP), but more drastically under former scenario. The significant increase in aerosol

336   pH with strict control policy will lead to more nitrate partitioning in aerosol phase, hence inhibiting future

337    $PM_{2.5}$ pollution control. This finding implicates that variations in aerosol pH will feedback to

338   multiphase formation pathways of aerosols in the atmosphere. In other words, proportional

339   reductions in precursors and follow-up variations in aerosol pH are evidently necessary to be taken into

340   account for future efforts in mitigating haze pollution.

341   **Author Contributions**

342   HS, HW, and CH conceived and led the study. MZ conducted the field measurements and carried out the

343   data analysis. MZ and GZ performed model simulations. MZ, HS, HW, CH, GZ, LQ, SZ, DH, YC, JA

344   discussed the results. LQ, SZ, DH, SL, ST, QW, RY, YM, CC conducted the measurements at the station.

345   MZ, HS and GZ wrote the manuscript with input from all co-authors.

346 **Supplement**

347 The supplement is available in a separate file.

348 **Competing interests**

349 The authors declare that they have no conflict of interest.

350 **Data availability**

351 The data presented in this paper are available upon request from Hang Su (h.su@mpic.de) and Cheng

352 Huang (huangc@saes.sh.cn).

353 **Acknowledgement**

354 This study was supported by the National Key Research and Development Program of China

355 (2018YFC0213800), Science and Technology Commission of Shanghai Municipality Fund Project

356 (20dz1204000), the General Fund of National Natural Science Foundation of China (21806108), the

357 National Natural Science Foundation of China (42061134008), the Shanghai Rising-Star Program

358 (19QB1402900) and Shanghai Municipal Bureau of Ecology and Environment Fund Project (2020-03).

359 **Reference**

360 Battaglia, M. A., Douglas, S., and Hennigan, C. J.: Effect of the Urban Heat Island on Aerosol pH,
361 Environmental Science & Technology, 51, 13095-13103, 10.1021/acs.est.7b02786, 2017.
362 Cai, S., Wang, Y., Zhao, B., Wang, S., Chang, X., and Hao, J.: The impact of the "Air Pollution Prevention
363 and Control Action Plan" on PM2.5 concentrations in Jing-Jin-Ji region during 2012-2020, Sci Total
364 Environ, 580, 197-209, 10.1016/j.scitotenv.2016.11.188, 2017.
365 Cheng, J., Su, J., Cui, T., Li, X., Dong, X., Sun, F., Yang, Y., Tong, D., Zheng, Y., Li, Y., Li, J., Zhang,
366 Q., and He, K.: Dominant role of emission reduction in PM2.5 air quality improvement in Beijing during
367 2013–2017: a model-based decomposition analysis, Atmospheric Chemistry and Physics, 19, 6125-6146,
368 10.5194/acp-19-6125-2019, 2019.
369 Cheng, Y., Zheng, G., Wei, C., Mu, Q., Zheng, B., Wang, Z., Gao, M., Zhang, Q., He, K., Carmichael,
370 G., Poscjl, U., and Su, H.: Reactive nitrogen chemistry in aerosol water as a source of sulfate during haze
371 events in China, Science Advance, 2016.
372 Clegg, S. L., Brimblecombe, P., and Wexler, A. S.: Thermodynamic Model of the System
373 $H^+-NH_4^+-Na^+-SO_4^{2-}-NO_3^--Cl^--H_2O$ at 298.15 K, The Journal of Physical Chemistry A, 102, 2155-
374 2171, 10.1021/jp973043j, 1998.
375 Ding, J., Zhao, P., Su, J., Dong, Q., Du, X., and Zhang, Y.: Aerosol pH and its driving factors in Beijing,
376 Atmospheric Chemistry and Physics, 19, 7939-7954, 10.5194/acp-19-7939-2019, 2019.
377 Fang, T., Guo, H., Zeng, L., Verma, V., Nenes, A., and Weber, R. J.: Highly Acidic Ambient Particles,
378 Soluble Metals, and Oxidative Potential: A Link between Sulfate and Aerosol Toxicity, Environ Sci

379   Technol, 51, 2611-2620, 10.1021/acs.est.6b06151, 2017.

380   Fountoukis, C. and Nenes, A.: ISORROPIA II: a computationally efficient thermodynamic equilibrium

381   model for K+–Ca2+–Mg2+–NH+4 –Na+–SO2− 4 –NO− 3 –Cl−–H2O aerosols, Atmospheric Chemistry

382   and Physics, 7, 4639-4659, 2007.

383   Fu, X., Guo, H., Wang, X., Ding, X., He, Q., Liu, T., and Zhang, Z.: PM2.5 acidity at a background site

384   in the Pearl River Delta region in fall-winter of 2007-2012, J Hazard Mater, 286, 484-492,

385   10.1016/j.jhazmat.2015.01.022, 2015.

386   Guo, H., Weber, R. J., and Nenes, A.: High levels of ammonia do not raise fine particle pH sufficiently

387   to yield nitrogen oxide-dominated sulfate production, Sci Rep, 7, 12109, 10.1038/s41598-017-11704-0,

388   2017a.

389   Guo, H., Otjes, R., Schlag, P., Kiendler-Scharr, A., Nenes, A., and Weber, R. J.: Effectiveness of ammonia

390   reduction on control of fine particle nitrate, Atmospheric Chemistry and Physics, 18, 12241-12256,

391   10.5194/acp-18-12241-2018, 2018.

392   Guo, H., Liu, J., Froyd, K. D., Roberts, J. M., Veres, P. R., Hayes, P. L., Jimenez, J. L., Nenes, A., and

393   Weber, R. J.: Fine particle pH and gas–particle phase partitioning of inorganic species in Pasadena,

394   California, during the 2010 CalNex campaign, Atmospheric Chemistry and Physics, 17, 5703-5719,

395   10.5194/acp-17-5703-2017, 2017b.

396   Guo, H., Sullivan, A. P., Campuzano-Jost, P., Schroder, J. C., Lopez-Hilfiker, F. D., Dibb, J. E., Jimenez,

397   J. L., Thornton, J. A., Brown, S. S., Nenes, A., and Weber, R. J.: Fine particle pH and the partitioning of

398   nitric acid during winter in the northeastern United States, Journal of Geophysical Research:

399   Atmospheres, 121, 10,355-310,376, 10.1002/2016jd025311, 2016.

400   Guo, H., Xu, L., Bougiatioti, A., Cerully, K. M., Capps, S. L., Hite, J. R., Carlton, A. G., Lee, S. H.,

401   Bergin, M. H., Ng, N. L., Nenes, A., and Weber, R. J.: Fine-particle water and pH in the southeastern

402   United States, Atmospheric Chemistry and Physics, 15, 5211-5228, 10.5194/acp-15-5211-2015, 2015.

403   He, P., Alexander, B., Geng, L., Chi, X., Fan, S., Zhan, H., Kang, H., Zheng, G., Cheng, Y., Su, H., Liu,

404   C., and Xie, Z.: Isotopic constraints on heterogeneous sulfate production in Beijing haze, Atmospheric

405   Chemistry and Physics, 18, 5515-5528, 10.5194/acp-18-5515-2018, 2018.

406   Hennigan, C. J., Izumi, J., Sullivan, A. P., Weber, R. J., and Nenes, A.: A critical evaluation of proxy

407   methods used to estimate the acidity of atmospheric particles, Atmospheric Chemistry and Physics, 15,

408   2775-2790, 10.5194/acp-15-2775-2015, 2015.

409   Huang, X. H. H., Bian, Q., Ng, W. M., Louie, P. K. K., and Yu, J. Z.: Characterization of PM2.5 Major

410   Components and Source Investigation in Suburban Hong Kong: A One Year Monitoring Study, Aerosol

411   and Air Quality Research, 14, 237-250, 10.4209/aaqr.2013.01.0020, 2014.

412   Jia, S., Wang, X., Zhang, Q., Sarkar, S., Wu, L., Huang, M., Zhang, J., and Yang, L.: Technical note:

413   Comparison and interconversion of pH based on different standard states for aerosol acidity

414   characterization, Atmospheric Chemistry and Physics, 18, 11125-11133, 10.5194/acp-18-11125-2018,

415   2018.

416   Li, C., Hu, Y., Chen, J., Ma, Z., Ye, X., Yang, X., Wang, L., Wang, X., and Mellouki, A.: Physiochemical

417   properties of carbonaceous aerosol from agricultural residue burning: Density, volatility, and

418   hygroscopicity, Atmospheric Environment, 140, 94-105, 10.1016/j.atmosenv.2016.05.052, 2016.

419   Li, H., Cheng, J., Zhang, Q., Zheng, B., Zhang, Y., Zheng, G., and He, K.: Rapid transition in winter

420   aerosol composition in Beijing from 2014 to 2017: response to clean air actions, Atmospheric Chemistry

421   and Physics, 19, 11485-11499, 10.5194/acp-19-11485-2019, 2019.

422   Li, W., Xu, L., Liu, X., Zhang, J., Lin, Y., Yao, X., Gao, H., Zhang, D., Chen, J., Wang, W., Harrison, R.

423   M., Zhang, X., Shao, L., Fu, P., Nenes, A., and Shi, Z.: Air pollution–aerosol interactions produce more
424   bioavailable iron for ocean ecosystems, Science Advance, 3, e1601749, 2017.

425   Liu, M., Huang, X., Song, Y., Xu, T., Wang, S., Wu, Z., Hu, M., Zhang, L., Zhang, Q., Pan, Y., Liu, X.,
426   and Zhu, T.: Rapid SO2 emission reductions significantly increase tropospheric ammonia concentrations
427   over the North China Plain, Atmospheric Chemistry and Physics, 18, 17933-17943, 10.5194/acp-18-
428   17933-2018, 2018.

429   Masiol, M., Squizzato, S., Formenton, G., Khan, M. B., Hopke, P. K., Nenes, A., Pandis, S. N., Tositti,
430   L., Benetello, F., Visin, F., and Pavoni, B.: Hybrid multiple-site mass closure and source apportionment
431   of PM2.5 and aerosol acidity at major cities in the Po Valley, Sci Total Environ, 704, 135287,
432   10.1016/j.scitotenv.2019.135287, 2020.

433   Nah, T., Guo, H., Sullivan, A. P., Chen, Y., Tanner, D. J., Nenes, A., Russell, A., Ng, N. L., Huey, L. G.,
434   and Weber, R. J.: Characterization of aerosol composition, aerosol acidity, and organic acid partitioning
435   at an agriculturally intensive rural southeastern US site, Atmospheric Chemistry and Physics, 18, 11471-
436   11491, 10.5194/acp-18-11471-2018, 2018.

437   Nenes, A., Pandis, S. N., Weber, R. J., and Russell, A.: Aerosol pH and liquid water content determine
438   when particulate matter is sensitive to ammonia and nitrate availability, Atmospheric Chemistry and
439   Physics, 20, 3249-3258, 10.5194/acp-20-3249-2020, 2020a.

440   Nenes, A., Pandis, S. N., Kanakidou, M., Russell, A., Song, S., Vasilakos, P., and Weber, R. J.: Aerosol
441   acidity and liquid water content regulate the dry deposition of inorganic reactive nitrogen, Atmospheric
442   Chemistry and Physics Discussion, 10.5194/acp-2020-266, 2020b.

443   Pye, H. O. T., Zuend, A., Fry, J. L., Isaacman-VanWertz, G., Capps, S. L., Appel, K. W., Foroutan, H.,
444   Xu, L., Ng, N. L., and Goldstein, A. H.: Coupling of organic and inorganic aerosol systems and the effect
445   on gas-particle partitioning in the southeastern US, Atmos Chem Phys, 18, 357-370, 10.5194/acp-18-
446   357-2018, 2018.

447   Pye, H. O. T., Nenes, A., Alexander, B., Ault, A. P., Barth, M. C., Clegg, S. L., Collett Jr, J. L., Fahey, K.
448   M., Hennigan, C. J., Herrmann, H., Kanakidou, M., Kelly, J. T., Ku, I. T., McNeill, V. F., Riemer, N.,
449   Schaefer, T., Shi, G., Tilgner, A., Walker, J. T., Wang, T., Weber, R., Xing, J., Zaveri, R. A., and Zuend,
450   A.: The acidity of atmospheric particles and clouds, Atmospheric Chemistry and Physics, 20, 4809-4888,
451   10.5194/acp-20-4809-2020, 2020.

452   Qiao, L., Cai, J., Wang, H., Wang, W., Zhou, M., Lou, S., Chen, R., Dai, H., Chen, C., and Kan, H.:
453   PM2.5 constituents and hospital emergency-room visits in Shanghai, China, Environ Sci Technol, 48,
454   10406-10414, 10.1021/es501305k, 2014.

455   Rumsey, I. C., Cowen, K. A., Walker, J. T., Kelly, T. J., Hanft, E. A., Mishoe, K., Rogers, C., Proost, R.,
456   Beachley, G. M., Lear, G., Frelink, T., and Otjes, R. P.: An assessment of the performance of the Monitor
457   for AeRosols and GAses in ambient air (MARGA): a semi-continuous method for soluble compounds,
458   Atmospheric Chemistry and Physics, 14, 5639-5658, 10.5194/acp-14-5639-2014, 2014.

459   Shi, X., Nenes, A., Xiao, Z., Song, S., Yu, H., Shi, G., Zhao, Q., Chen, K., Feng, Y., and Russell, A. G.:
460   High-Resolution Data Sets Unravel the Effects of Sources and Meteorological Conditions on Nitrate and
461   Its Gas-Particle Partitioning, Environ Sci Technol, 53, 3048-3057, 10.1021/acs.est.8b06524, 2019.

462   Song, S., Gao, M., Xu, W., Shao, J., Shi, G., Wang, S., Wang, Y., Sun, Y., and McElroy, M. B.: Fine-
463   particle pH for Beijing winter haze as inferred from different thermodynamic equilibrium models,
464   Atmospheric Chemistry and Physics, 18, 7423-7438, 10.5194/acp-18-7423-2018, 2018.

465   Su, H., Cheng, Y., and Poschl, U.: New Multiphase Chemical Processes Influencing Atmospheric
466   Aerosols, Air Quality, and Climate in the Anthropocene, Acc Chem Res, 53, 2034-2043,

467 10.1021/acs.accounts.0c00246, 2020.

468 Tan, T., Hu, M., Li, M., Guo, Q., Wu, Y., Fang, X., Gu, F., Wang, Y., and Wu, Z.: New insight into PM2.5
469 pollution patterns in Beijing based on one-year measurement of chemical compositions, Sci Total
470 Environ, 621, 734-743, 10.1016/j.scitotenv.2017.11.208, 2018.

471 Tao, W., Su, H., Zheng, G., Wang, J., Wei, C., Liu, L., Ma, N., Li, M., Zhang, Q., Pöschl, U., and Cheng,
472 Y.: Aerosol pH and chemical regimes of sulfate formation in aerosol water during winter haze in the
473 North China Plain, Atmospheric Chemistry and Physics, 20, 11729-11746, 10.5194/acp-20-11729-2020,
474 2020.

475 Tao, Y. and Murphy, J. G.: The sensitivity of PM2.5 acidity to meteorological parameters and chemical
476 composition changes: 10-year records from six Canadian monitoring sites, Atmos. Chem. Phys., 19,
477 9309-9320, 10.5194/acp-19-9309-2019, 2019.

478 Tong, D., Cheng, J., Liu, Y., Yu, S., Yan, L., Hong, C., Qin, Y., Zhao, H., Zheng, Y., Geng, G., Li, M.,
479 Liu, F., Zhang, Y., Zheng, B., Leon, C., and Zhang, Q.: Dynamic projection of anthropogenic emissions
480 in China: methodology and 2015–2050 emission pathways under a range of socio-economic, climate
481 policy, and pollution control scenarios, Atmospheric Chemistry and Physics, 20, 5729-5757,
482 10.5194/acp-20-5729-2020, 2020.

483 Wang, H., Ding, J., Xu, J., Wen, J., Han, J., Wang, K., Shi, G., Feng, Y., Ivey, C. E., Wang, Y., Nenes, A.,
484 Zhao, Q., and Russell, A. G.: Aerosols in an arid environment: The role of aerosol water content,
485 particulate acidity, precursors, and relative humidity on secondary inorganic aerosols, Sci Total Environ,
486 646, 564-572, 10.1016/j.scitotenv.2018.07.321, 2019.

487 Wang, S., Wang, L., Li, Y., Wang, C., Wang, W., Yin, S., and Zhang, R.: Effect of ammonia on fine-
488 particle pH in agricultural regions of China: comparison between urban and rural sites, Atmospheric
489 Chemistry and Physics, 20, 2719-2734, 10.5194/acp-20-2719-2020, 2020.

490 Weber, R. J., Guo, H., Russell, A. G., and Nenes, A.: High aerosol acidity despite declining atmospheric
491 sulfate concentrations over the past 15 years, Nature Geoscience, 9, 282-285, 10.1038/ngeo2665, 2016.

492 Xie, Y., Wang, G., Wang, X., Chen, J., Chen, Y., Tang, G., Wang, L., Ge, S., Xue, G., Wang, Y., and Gao,
493 J.: Nitrate-dominated PM2.5 and elevation of particle pH observed in urban Beijing during the winter of
494 2017, Atmospheric Chemistry and Physics, 20, 5019-5033, 10.5194/acp-20-5019-2020, 2020.

495 Zheng, B., Tong, D., Li, M., Liu, F., Hong, C., Geng, G., Li, H., Li, X., Peng, L., Qi, J., Yan, L., Zhang,
496 Y., Zhao, H., Zheng, Y., He, K., and Zhang, Q.: Trends in China's anthropogenic emissions since 2010 as
497 the consequence of clean air actions, Atmospheric Chemistry and Physics, 18, 14095-14111,
498 10.5194/acp-18-14095-2018, 2018.

499 Zheng, G., Su, H., Wang, S., Andreae, M. O., Poschl, U., and Cheng, Y.: Multiphase buffer theory
500 explains contrasts in atmospheric aerosol acidity, Science 369, 1374-1377, 2020.

501 Zhou, M., Qiao, L., Zhu, S., Li, L., Lou, S., Wang, H., Wang, Q., Tao, S., Huang, C., and Chen, C.:
502 Chemical characteristics of fine particles and their impact on visibility impairment in Shanghai based on
503 a 1-year period observation, J Environ Sci, 48, 151-160, 10.1016/j.jes.2016.01.022, 2016.

504